

# Modeling of a Glow Discharge in a Coaxial System of Electrodes


O. V. Andrienko<sup>f</sup>,  [0000-0001-9930-4415](https://orcid.org/0000-0001-9930-4415)

S. B. Sydorenko<sup>f</sup>,  [0000-0002-3109-2011](https://orcid.org/0000-0002-3109-2011)

S. O. Maikut, PhD,  [0000-0002-0913-4190](https://orcid.org/0000-0002-0913-4190)

L. Yu. Tsybulsky, PhD Assoc.Prof.,  [0000-0002-7431-6417](https://orcid.org/0000-0002-7431-6417)

A. I. Kuzmichev<sup>s</sup>, Dr.Sc.(Eng.) Prof.,  [0000-0003-0087-275X](https://orcid.org/0000-0003-0087-275X)

National Technical University of Ukraine "Igor Sikorsky Kyiv Polytechnic Institute"  [00syn5v21](https://www.researchgate.net/publication/358005951)  
Kyiv, Ukraine

**Abstract**—Modeling of a glow discharge in a cylindrical coaxial system with dielectric ends of electrodes in the hydrodynamic drift-diffusion approximation was performed. Model parameters: outer cathode diameter 10 and 13 mm, anode diameter 2 mm, voltage 2800 V, gas temperature 300 K.  $pd \sim 1$  Pa·m, which corresponds to the left side of the minimum area of the Paschen curve for discharge ignition. Reactions of ionization of atoms by electron impact, generation and quenching of metastable atoms, elastic collision of electrons with atoms and elastic collision of ions, resonant recharging of ions, Penning ionization, as well as secondary ion-electron emission of the cathode were taken into account. The distribution of potential and concentration of charged particles in the interelectrode space, the density of ion and electron currents were calculated within the framework of a self-consistent problem, and the current-voltage characteristics for two modes of discharge - plasma and plasma-free - were presented. The effect of  $pd$  on the parameters and discharge mode is determined. The obtained results can be used in plasma technologies for modification of the internal surfaces of metal, hollow, long parts with a small cross-sectional size, that is, in conditions close to those complicated by the occurrence of a discharge.

**Keywords** — glow discharge; diffusion models; plasma simulation.

## I. INTRODUCTION

Many electronic and photonic devices, as well as ion-plasma technologies, are based on various types of gas discharges. Among them, the anomalous glow discharge is the most widely used, and a lot of scientific and technical literature is devoted to it [1]-[4]. However, there are configurations of electrode systems that have not been studied much due to their specificity, they include the coaxial system in long tubes of small diameter, despite the fact that many tubular products require ion-plasma treatment of the inner surface [5]-[8].

It is quite difficult to experimentally study the discharge in such systems, especially the internal structure, that is, the distribution of the electric field, the concentration of charged particles, etc. Therefore, it is more expedient to use modelling methods, but those that allow the study of electrode systems with a high accuracy of description of the most important physical processes to obtain results that correspond to the actual characteristics of the system under study. The purpose of the work is to investigate the characteristics of a stable (non-oscillatory) glow discharge in a long coaxial system

of small-diameter electrodes at  $pd \sim 1$  Pa·m (where  $p$  is the working gas pressure, and  $d$  is the distance between the electrodes) on the model, which corresponds to the left part of the region of the minimum of the Paschen curve for discharge ignition [1], that is, in conditions where they provide both minimum energy consumption for discharge support and low  $pd$  values, which minimize collisions of ions with gas molecules and their loss of energy during collisions. This provides an effective kinetic influence of ions on the cathode surface and is used in most ionic technologies.

## II. OBJECT AND METHOD OF RESEARCH

The simulation was carried out for a coaxial cylindrical system with an external cathode and argon filling. The system of electrodes is shown in Fig. 1 and has the following parameters:

- inner radius of the cathode – 10 or 13 mm ( $r_c$ );
- external radius of the anode – 2 mm ( $r_a$ );
- axial length along the electrode system – 280 ( $L$ ) mm.



The electrode system was connected to DC voltage source  $\mathcal{E} = 2800$  V through a ballast resistor  $R_b$  (10-300 k $\Omega$ ), the value of which controls the discharge current. The pressure of argon (temperature – 300 K) corresponds to the above values  $pd = p(r_c - r_a)$ .

The following physical discharge model was chosen for the study: the physical processes (reactions) occur in the interelectrode gap, as presented in Table 1. Electrons are emitted from the cathode due to secondary ion-electron emission (coefficient  $\gamma = 0.1$ ), the electrodes collect charged particles falling on them without reflecting them. The ends of the system are closed by dielectric walls. The following processes are taken into account, which play the most important role in argon at a given  $pd$  range [3].

To model the glow discharge, we will use the hydrodynamic approach in the drift-diffusion approximation, which is simpler than the methods based on physical kinetics with the solution of the Boltzmann equation, and, as shown in literature [10]-[13], it gives physically correct results within the specified  $pd$  range. For the calculations based on the chosen model of glow discharge in a coaxial electrode system, a standard system of equations for the drift-diffusion approximation was used, which were adapted for a cylindrical coaxial system with dielectric ends and calculate the particle interaction processes from Table 1.

In the initial conditions, the initial density of electrons in the interelectrode space is set at the level of  $n_{e0} = 10^{13}$  m $^{-3}$ . A computer code similar to that described in [14]-[16] was used to solve the system of equations.

TABLE 1 REACTIONS DURING PARTICLE COLLISIONS

Reaction	Type of reaction
$e + \text{Ar} \rightarrow e + \text{Ar}$	Elastic collision of electrons with atoms
$e + \text{Ar} \leftrightarrow e + \text{Ar}^*$	Generation and quenching of a metastable atom under the action of an electron impact
$e + \text{Ar} \rightarrow 2e + \text{Ar}^+$	Ionization of atoms by electron impact
$\text{Ar}^+ + \text{Ar} \rightarrow \text{Ar}^+ + \text{Ar}$	Elastic collision of ions
$\text{Ar}^+ + \text{Ar} \rightarrow \text{Ar} + \text{Ar}^+$	Resonant recharging of ions
$\text{Ar}^* + \text{Ar}^* \rightarrow e + \text{Ar} + \text{Ar}^+$	Penning ionization
$\text{Ar}^* + \text{Ar} \rightarrow \text{Ar} + \text{Ar}$	Quenching of metastable atoms

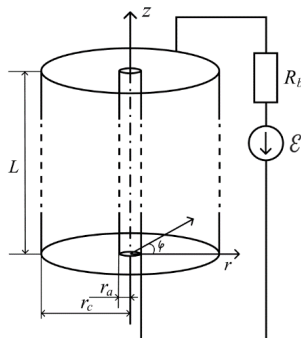


Fig. 1 Model of the discharge system

### III. SIMULATION RESULTS

In Fig. 2-4 show the graphs of potential distributions and the concentration of charged particles in the interelectrode gap (along  $r$ ). The regime of discharge existence was set using a ballast resistor  $R_b$ , and, accordingly, its value influences the discharge current and other characteristics. The discharge voltage, depending on the radius of the cathode (10 and 13 mm), was in the range of 115-155 V.

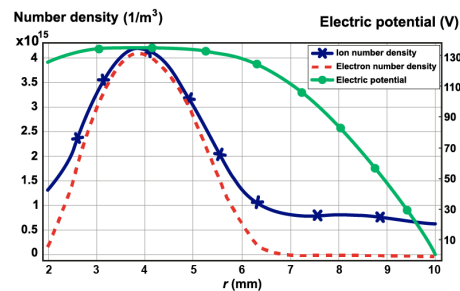


Fig. 2. Distribution of the potential and concentration of ions and electrons radially along the gap from the anode to the cathode in the middle of the electrode system  $r_c = 10$  mm,  $R_b = 50$  k $\Omega$ ,  $p = 133$  Pa.  $p \times (r_c - r_a) = 1.064$  Pa·m

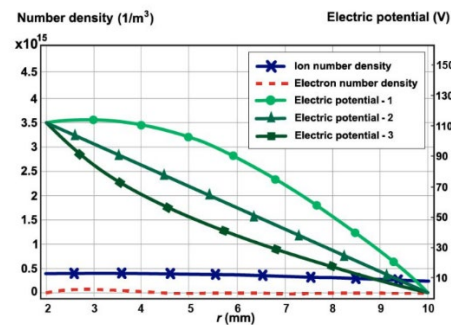


Fig. 3 Distribution of the potential and concentration of ions and electrons radially along the gap from the anode to the cathode in the middle of the electrode system.  $r_c = 10$  mm,  $R_b = 300$  k $\Omega$ .  $p = 133$  Pa.  $p \times (r_c - r_a) = 1.064$  Pa·m. Potential distribution in a cylindrical electrode system with a discharge - 1, without a discharge - 3, in a plane-parallel electrode system without a discharge - 2.

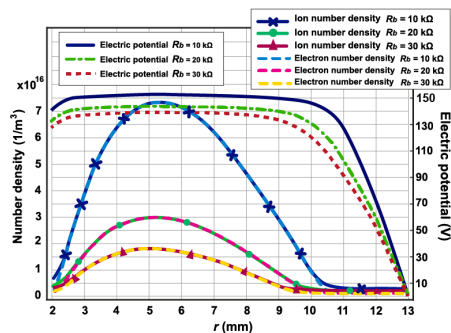


Fig. 4 Distribution of potential, density of ions and electrons radially along the gap from the anode to the cathode in the middle of the electrode system  $r_c = 13$  mm,  $R_b = 10, 20, 30$  k $\Omega$ .  $p = 1.33$  Pa·m.  $p \times (r_c - r_a) = 1.46$  Pa·m



In Fig. 2 shows the distribution of the potential in the case of the existence of plasma in the discharge gap, in Fig. 3 - in the absence of plasma. In both cases, the positive space charge of ions plays a significant role in the formation of the potential distribution curve in the interelectrode gap. It is known that the potential distribution in the coaxial system (vacuum capacitor) is characterized by strong heterogeneity, i.e. the electric field strength near the small-diameter inner electrode increases significantly in relation to the strength near the outer electrode in comparison with the constant field strength for plane-parallel electrodes. These features lead to different distributions of potentials in vacuum coaxial and planar systems, and their difference from the distribution in the presence of spatial ion charge is also shown (Figs. 2, 3).

In Fig. 5 shows the distribution of the ion current density  $j_c$  along the surface of the cathode. The current density is uniform along the surface (except for  $R_b = 300 \text{ k}\Omega$ ,  $r_c = 10 \text{ mm}$  for a very low-current discharge) and is  $0.6 - 1.1 \text{ A/m}^2$ .

To analyze the characteristics of the discharge in the system under investigation, it is desirable to use the current-voltage characteristics (I-V curve) of the discharge, because they are commonly used in the literature. However, the calculated total current includes the part that is ambiguously influenced by the dielectric ends of the electrode system. Therefore, the modified I-V characteristics are presented in the form of "discharge voltage - current density at the anode (Fig. 6) ion discharge current density at the cathode (Fig. 7) in the central part of the system." In the field of Figs. 6, 7, the values of the ballast resistor for plotting individual I-V curve points are indicated. The presented characteristics are calculated for different values of the interelectrode gap (at  $r_c = 10 \text{ mm}$ , the gap is  $8 \text{ mm}$ , and at  $r_c = 13 \text{ mm}$ , it is  $11 \text{ mm}$ ).

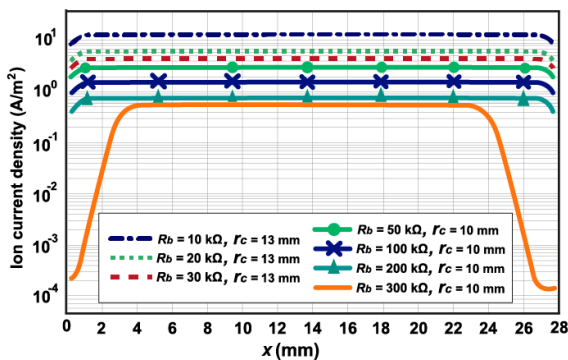


Fig. 5 Graph of the distribution of the ion current density on the cathode along its surface. Ballast resistance values from top to bottom, k $\Omega$ : 10, 20, 30, 50, 100, 200, 300.  $r_c = 10 \text{ mm}, 13 \text{ mm}$ .  $p = 133 \text{ Pa}$ .  $p \times (r_c - r_a) = 1.064$  and  $1.463 \text{ Pa}\cdot\text{m}$

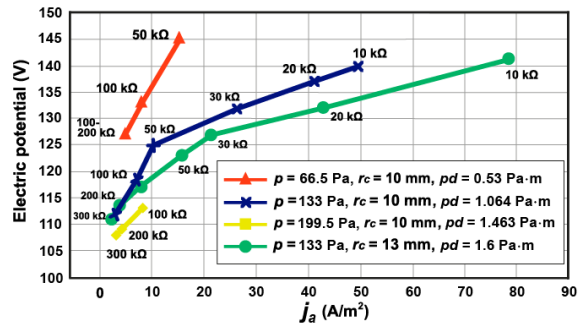


Fig. 6 I-V curve characteristic of the discharge at different pressures for the anode

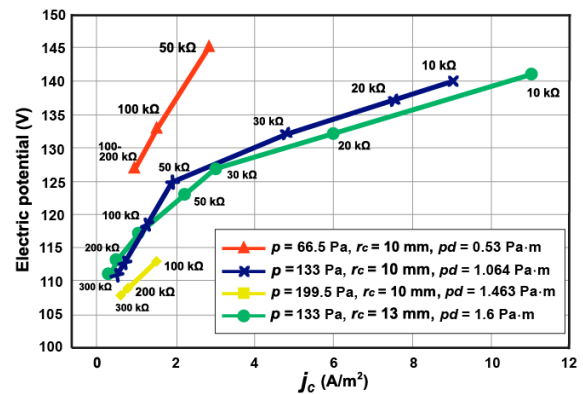


Fig. 7 I-V curve of the discharge at different pressures for the cathode

#### IV. DISCUSSION OF SIMULATION RESULTS

As a result of the simulation, data were obtained indicating that the discharge at  $pd$ , which is typical for the left part of the region of minimum of the Paschen curves, where the discharge voltage begins to rise, has all the features of a typical glow discharge, but with the specifics of different states (modes). In all modes, ion-electron emission and electron impact ionization are present, and the discharge voltage corresponds to the typical value for a glow discharge [3]. The essential role of the spatial charge of ions leads to a nonlinear potential distribution even at low current densities ( $\sim 80 \mu\text{A/cm}^2$  for  $R_b = 300 \text{ k}\Omega$ , Fig. 3, Fig. 7). The nature of the potential distribution indicates the formation of a space charge of ions in the interelectrode gap near the cathode layer, in which ion generation takes place.

At low currents and  $pd$ , the ion layer extends from the cathode to the anode with a slow increase in the concentration of ions (Fig. 3), and the electron concentration  $n_e$  is less than the ion concentration  $n_p$  by a factor of  $\sim \gamma$ , which indicates the absence of plasma formation in the gap. Such a plasma-free mode of discharge is called the simplest or Townsend mode in the literature [5,13]. It has a linear potential distribution (curve 2 in Fig. 3) and constant electric field strength due to the minimal influence of the space ion charge. However, in our case,



the plasma-free discharge mode has a non-linear potential distribution (curve 1 in Fig. 3) due to the strong influence of the space ion charge, but this mode will also be classified as the simplest. Its feature is the positive slope of the I–V curve. We also note that the space ion charge neutralizes the effect of the coaxiality geometry of the electrode system with increased field strength near the inner electrode (compare curves 1 and 3 in Fig. 3).

I–V curve for  $R_b = 300, 100, 50 \text{ k}\Omega$  in Fig. 6, 7 for  $r_c = 10, 13 \text{ mm}$  ( $pd = 0.53, 1.064, 1.463 \text{ Pa}\cdot\text{m}$ ) just refer to the simplest plasma-free mode. In this mode, the difference between the concentrations of electrons and ions decreases with a decrease in the ballast resistance  $R_b$ , i.e., with an increase in the discharge current. However, even with  $R_b = 50 \text{ k}\Omega$  ( $pd = 1.064 \text{ Pa}\cdot\text{m}$ ) and  $R_b = 100 \text{ k}\Omega$  ( $pd = 1.6 \text{ Pa}\cdot\text{m}$ ), complete equality is not achieved between the concentrations of electrons and ions in the region of the maximum concentration of charged particles (Fig. 2).

In the gap between the cathode and the anode, the potential distribution has a near-cathode part with a potential increase ( $\sim 130 \text{ V}$ , for  $j_c \sim 3 \text{ A/m}^2$ ), and then a decrease in the near-anode region ( $\sim 15 \text{ V}$ ). The transition from one part of the distribution to another is in the region of the maximum concentration of charged particles (at  $r = 4 \text{ mm}$ , Fig. 2). In this plasma-free mode of discharge, two ion shells are created with a predominance of ion concentration.

A different situation is observed with a decrease in  $R_b$  (30, 20, 10 kΩ) on the I–V curve of Fig. 6, 7. The curves decrease the angle of inclination, both for  $r_c = 10 \text{ mm}$  and for 13 mm. The transfers to another mode. There is an equalization of the concentrations of electrons and ions between the cathode and the anode, that is, a plasma of negative glow is formed, as in a typical glow discharge (Fig. 4). In addition, the potential distribution has three parts: a cathodic fall with a rapid increase in potential (130–150 V,  $j_c > 3 \text{ A/m}^2$ ), a fall in the negative glow region with a weak increase (up to 5 V) and an anodic fall with a weak decrease ( $\sim 15 \text{ V}$ ). In this way, two near-electrode shells are created with a predominance of ion concentration.

The fall in the region of negative glow for this mode is characterized by an increase in the region itself and the concentration of charged particles in it with increasing current density.

The density distribution of ions and electrons in the radial direction is somewhat reminiscent of the solution of the diffusion equation for the lower diffusion mode, [4]. The maximum concentration creates a ring around the anode, and the minimum concentration is near the cathode.

Discharges in coaxial systems are characterized by different current densities for the internal (in our case,

the anode) and external (cathode) electrodes, which are connected through the secondary emission coefficient and the geometry influence coefficient, i.e. the ratio of the areas (radii) of the electrodes.

$$j = \frac{j_i \cdot (1 + \gamma) \cdot R_c}{R_a}$$

For a plane-parallel electrode system, the geometry influence coefficient  $R_c/R_a$  disappears. For our coaxial case,  $R_c/R_a = 10/2, 13/2 = 5, 6.5$ , that is, the geometry of the system has some influence on the processes in the near-electrode regions.

The near-anode distortion of the field begins at a distance of  $\sim 1 \text{ mm}$  from the anode with a radius of 2 mm, but these values are of the same order, so it can be considered that the thickening of the line on the anode is not significantly greater than in the plane-parallel system, but the thickening of the field lines and, accordingly, the increase in the current density on anode, creates a situation where it is necessary to balance the currents of the cathode and anode due to the reduction of the voltage between the plasma and the anode. Due to the smaller area, the anode cannot receive as many electrons that come from the plasma cathode [17] [19], and therefore in the ion shell around the anode, electrons begin to accumulate to limit the flow of electrons from the plasma to the anode. Since the anodic voltage drop prevents the movement of a part of electrons with an energy lower than  $\sim 15 \text{ eV}$  for both cathode radii, it can be assumed that the average energy of electrons in the near-anode region is of the order of this value.

The distribution of charged particles around the anode and the radial distribution of the potential show that in the plasma mode, the plasma is concentrated in the region of maximum charged particle concentration, where their main generation and diffusion occurs with subsequent deionization at the electrodes. It is important to note that the potential drop in the near-anode region does not hinder with the diffusion movement of ions.

The discharge is considered obstructed if the length of the cathode fall is greater or equal to the interelectrode distance [18]. In Fig. 3, the electric field potential curve rises monotonically almost to the anode, and the plasma region does not exist. On the I–V curve of Fig. 6, 7 this refers to the steeper parts of the curves, located to the left of the "fracture", where we have a discharge in a complicated form or close to it. In the right parts of the curves, relative to the "fracture", a plasma region appears, which expands with an increase in the parameter  $p \times (r_c - r_a)$ . and the distance between the cathode and the anode, while the maximum concentration of charged particles moves away from the anode (Figs. 2, 3), and we can no longer speak of a obstructed form.





## CONCLUSIONS

A physics-topological and topological model of a low-pressure glow discharge in the  $pd$  range from 0.53 to 1.6 Pa·m in an extended coaxial system ( $r \ll L$ ) with a small-diameter external cathode was constructed. As a result, different glow discharge modes are observed — plasma-free and plasma, which differ in the following.

The conditions for the occurrence of the discharge correspond to the left part of the region of the minimum of the Paschen curve within the framework of the drift-diffusion approximation, which made it possible to identify the peculiarities of the discharge in an extended coaxial system ( $r \ll L$ ) with an external cathode of a small diameter in comparison with the discharge in a plane-parallel system of electrodes.

The plasma-free mode is observed at a low current density (at the cathode  $\sim 0.6 \dots 2 \text{ A/m}^2$ ) and has a steeply increasing I–V curve. The plasma mode at a higher current density has a much slope I–V curve with a smaller angle of inclination. The transition from one mode to another occurs at cathode current densities  $\sim 1.8 \dots 2.5 \text{ A/m}^2$ . In the mentioned range of  $pd$ , the discharge form characteristic of the normal glow discharge shape is not observed.

For the plasma-free mode, the length of the cathode fall approaches the interelectrode distance. Such a discharge mode is often called obstructed, since there is no region of negative glow characteristic of a glow discharge, in which the main amount of ions is actually generated, part of which drifts to the cathode and causes secondary ion-electron emission.

In contrast to the plasma-free form of discharge in a coaxial system of electrodes, plasma-free discharge between planar electrodes at similar  $pd$  (i.e., dark discharge or Townsend discharge), as is known, has a horizontal I–V curve, as it is maintained at a voltage approaching to the voltage at which the discharge occurs.

In the plasma mode of the discharge in the given range  $pd$ , the plasma discharge region is a region of plasma of negative glow, which extends from the region of the cathodic potential fall to the region of the anodic fall. The plasma discharge mode in the coaxial system

resembles the anomalous form of the glow discharge between planar electrodes at similar  $pd$ .

There are ion shells around both electrodes in the plasma mode. The cathode ion sheath provides secondary cathode emission due to ion bombardment and acceleration of electrons to the energy required for gas ionization. The existence of an ion shell around the anode is due to the high density of electrons around it and the automatic creation of a braking field for excess electrons. In this way, the equality of the total currents (ions and electrons) on both electrodes and in the gap is maintained in the discharge.

A feature of discharge in a coaxial system with an internal anode is a significant increase in the discharge current density at the anode compared to the current density at the cathode. The increase in density is proportional to the ratio of the cathode and anode radii.

In both modes of discharge, the electron and ion concentration distributions in the gap have a significantly non-homogeneous dome-like character with a shift of the maximum towards the anode. The dome-shaped nature of the distribution is due to the movement of ions to the electrodes due to diffusion and drift in the electric field with subsequent recombination (the maximum potential of space occurs in the region of the maximum concentration of charged particles, and the electric field vector is directed to both electrodes).

With an increase in the parameter  $pd$  and the distance between the cathode and the anode, the region of gas ionization, including the region of the negative glow plasma, expands, and the maximum of the distribution shifts away from the anode.

Thus, the studies showed that in the plasma mode of the glow discharge in the coaxial electrode system at  $pd = 1$  and  $1.5 \text{ Pa/m}$  in argon, the maximum ion current density at the cathode is  $9$  and  $11 \text{ A/m}^2$ , and the maximum concentration of charged particles in of the interelectrode gap is  $\sim 7 \cdot 10^{15} \text{ m}^{-3}$  at a discharge voltage of  $140 \text{ V}$ .

The obtained results can be used in the development of plasma technologies for the modification of the internal surfaces of metal hollow elongated parts with a small cross-sectional size.

## REFERENCES

- [1]. Y. P. Raizer "Gas Discharge Physics, J. E. Allen ed., Heidelberg: Springer Berlin, 1991. ISBN: 978-3-642-64760-4
- [2]. B. N. Klyarfeld, L. G. Guseva, and F. S. Pokrovskaya-Soboleva, "Glow discharge at low pressures and current density up to  $0.1 \text{ A/cm}^2$  [Tleyushchiy razryad pri nizkikh davleniyah i plotnostyah toka do  $0.1 \text{ A/cm}^2$ ]", Zhurnal Tehn. Fiziki, vol. 36, no. 4, pp. 704–713, Jan. 1966.
- [3]. A. Fridman and L. A. Kennedy, 3rd ed. Third edition. | Boca Raton : CRC Press, 2021.: CRC Press, 2021. DOI: 10.1201/9781315120812
- [4]. J. Reece Roth, "Industrial Plasma Engineering: Volume 1: Principles" (1st ed.), CRC Press, 1995. DOI: 10.1201/9780367802615
- [5]. T. Aizawa and K. Wasa, "Low Temperature Plasma Nitriding of Inner Surfaces in Stainless Steel Mini-/Micro-Pipes and Nozzles", Micromachines, vol. 8, no. 5, p. 157, May 2017. DOI: 10.3390/mi8050157



- [6]. H. Aghajani and S. Behrang, "Plasma Nitriding of Steels," Cham: Springer International Publishing, 2017. DOI: 10.1007/978-3-319-43068-3
- [7]. P. Phadke, J. M. Sturm, R. W. van de Kruijs, and F. Bijkerk, "Sputtering and nitridation of transition metal surfaces under low energy, steady state nitrogen ion bombardment", Applied Surface Science, vol. 505, p. 144529, Mar. 2020. DOI: 10.1016/j.apsusc.2019.144529
- [8]. A. Kuzmichev, V. Perevertaylo, L. Tsybulsky, and O. Volpian, "Characteristics of flows of energetic atoms reflected from metal targets during ion bombardment", Journal of Physics: Conference Series, vol. 729, p. 012005, Jul. 2016. DOI: 10.1088/1742-6596/729/1/012005
- [9]. V. A. Lisovskiy and S. D. Yakovin, "Experimental study of a low-pressure glow discharge in air in large-diameter discharge tubes: I. conditions for the normal regime of a glow discharge", Plasma Physics Reports, vol. 26, no. 12, pp. 1066–1075, Dec. 2000. DOI: 10.1134/1.1331142
- [10]. A. Bouchikhi, "Two-Dimensional Numerical Simulation of the DC Glow Discharge in the Normal Mode and with Einstein's Relation of Electron Diffusivity", Plasma Science and Technology, vol. 14, no. 11, pp. 965–973, Nov. 2012. DOI: 10.1088/1009-0630/14/11/04
- [11]. P. G. C. Almeida, M. S. Benilov, and M. J. Faria, "Study of stability of dc glow discharges with the use of Comsol Multiphysics software", Journal of Physics D: Applied Physics, vol. 44, no. 41, p. 415203, Sep. 2011. DOI: 10.1088/0022-3727/44/41/415203
- [12]. P. G. C. Almeida and M. S. Benilov, "Multiple solutions in the theory of near-cathode layers and self-organization on DC glow cathodes", in 2008 IEEE 35th International Conference on Plasma Science, Karlsruhe, Germany, 2008, pp. 1–1. DOI: 10.1109/PLASMA.2008.4591201.
- [13]. R. Kumar, R. Narayanan, R. D. Tarey, and A. Ganguli, "Characterization of DC glow discharge plasma in co-axial electrode geometry system by nonlinear dynamical analysis tools", Physics of Plasmas, vol. 30, no. 1, Jan. 2023. DOI: 10.1063/5.0111124
- [14]. A. Bouchikhi and A. Hamid, "2D DC Subnormal Glow Discharge in Argon", Plasma Science and Technology, vol. 12, no. 1, pp. 59–66, Feb. 2010. DOI: 10.1088/1009-0630/12/1/13
- [15]. Plasma Module User's Guide, pp. 76-83. COMSOL Multiphysics® v. 6.2. COMSOL AB, Stockholm, Sweden. 2023 URL: <https://doc.comsol.com/6.2/doc/com.comsol.help.plasma/PlasmaModuleUsersGuide.pdf>
- [16]. G. J. M. Hagelaar and L. C. Pitchford, "Solving the Boltzmann equation to obtain electron transport coefficients and rate coefficients for fluid models", Plasma Sources Science and Technology, vol. 14, no. 4, pp. 722–733, Oct. 2005. DOI: 10.1088/0963-0252/14/4/011
- [17]. A. I. Kuzmichev, "Gas discharge systems with secondary emitters for electronic equipment", Kyiv, 2018, p. 425.
- [18]. A. Bogaerts and R. Gijbels, "Numerical modelling of gas discharge plasmas for various applications", Vacuum, vol. 69, no. 1-3, pp. 37–52, Dec. 2002. DOI: 10.1016/S0042-207X(02)00306-8
- [19]. Surzhikov S.T. Computational Physics of Electric Discharges in Gas Flows (De Gruyter Studies in Mathematical Physics, 7). Walter de Gruyter GmbH, Berlin/Boston. 2012. 439 p. ISBN: 9783110270334

Надійшла до редакції 02 серпня 2024 року

Прийнята до друку 25 жовтня 2024 року





# Моделювання тліючого розряду в коаксіальній системі електродів

О. В. Андрієнко<sup>f</sup>,  [0000-0001-9930-4415](https://orcid.org/0000-0001-9930-4415)


С. Б. Сидоренко<sup>f</sup>,  [0000-0002-3109-2011](https://orcid.org/0000-0002-3109-2011)

С. О. Майкут, PhD,  [0000-0002-0913-4190](https://orcid.org/0000-0002-0913-4190)

Л. Ю. Цибульський, канд. техн. наук доц.,  [0000-0002-7431-6417](https://orcid.org/0000-0002-7431-6417)

А. І. Кузьмичев<sup>s</sup>, д-р техн. наук проф.,  [0000-0003-0087-275X](https://orcid.org/0000-0003-0087-275X)

Національний технічний університет України

«Київський політехнічний інститут імені Ігоря Сікорського»  [00syn5v21](https://ror.org/00syn5v21)

Київ, Україна

**Abstract**—Виконано моделювання тліючого розряду в циліндричній коаксіальній системі з діелектричними торцями електродів в гідродинамічному дрейфово-дифузному наближенні. Параметри моделі: діаметр зовнішнього катода 10 та 13 мм, діаметр анода 2 мм, напруга 2800 В, температура газу 300 К.  $pd \sim 1$  Па·м, що відповідає лівій частині області мінімуму кривої Пашена для запалювання розряду. Були враховані реакції іонізації атомів електронним ударом, генерації та гасіння метастабільних атомів, пружного зіткнення електронів з атомами та пружне зіткнення іонів, резонансне перезарядження іонів, іонізація Пенінга, а також вторинна іонно-електронна емісія катода. Були розраховані в рамках самоузгодженої задачі розподіл потенціалу і концентрації заряджених частинок в міжелектродному проміжку, густини іонних і електронних струмів, представлені вольт-амперні характеристики для двох мод розряду - плазмового та безплазмового. Визначено вплив  $pd$  на параметри та моду розряду. Отримані результати можуть бути використані в плазмових технологіях модифікації внутрішніх поверхонь металевих, порожнистих, протяжних деталей з малим поперечним розміром, тобто в умовах близьких до ускладненого виникненням розряду.

**Ключові слова** — тліючий розряд; дифузійні моделі; моделювання плазми.

